

Rapid prototyping of a Cyclic Olefin Co-polymer microfluidic device for automated oocyte culturing

Miguel Berenguel-Alonso,¹ Maria Sabés-Alsina,² Roser Morató,³ Oriol Ymbern,¹ Laura Rodríguez-Vázquez,² Oriol Talló-Parra,² Julián Alonso-Chamarro,¹ Mar Puyol¹ and Manel López-Béjar²

¹ *Group of Sensors and Biosensors, Chemistry Department, Universitat Autònoma de Barcelona, Bellaterra, 08193, Spain*

² *Department of Animal Health and Anatomy, Universitat Autònoma de Barcelona, 08193 Bellaterra, Spain*

³ *Biotechnology of Animal and Human Reproduction (TechnoSperm), Department of Biology, Institute of Food and Agricultural Technology, University of Girona, E-17071 Girona, Spain*

Miguel Berenguel-Alonso and Maria Sabés-Alsina contributed equally to this work

Corresponding Authors:

Mar Puyol,

e-mail: mariadelmar.puyol@uab.es

tel: +34 935868296

fax: +34 935812379

Manel López-Béjar,

e-mail: manel.lopez.bejar@uab.cat

tel: +34 935814615

fax: +34 935812006

The total number of words of the manuscript, including entire text from title page to figure legends: **7347**

The number of words of the abstract: **190**

The number of figures: **6**

The number of tables: **2**

Abstract

Assisted Reproductive Technology (ART) can benefit from the features of microfluidic technologies such as the automation of time-consuming labor-intensive procedures, the possibility to mimic *in vivo* environments and the miniaturization of the required equipment. To date, most of the proposed approaches are based on polydimethylsiloxane (PDMS) as platform substrate material due to its widespread use in academia, despite certain disadvantages such as the elevated cost of mass production. Herein, we present a rapid fabrication process for a Cyclic Olefin Co-polymer (COC) monolithic microfluidic device combining hot embossing –using a Low Temperature Co-fired Ceramic (LTCC) master– and micromilling. The microfluidic device was suitable for trapping and maturation of bovine oocytes, which were further studied to determine their ability to be fertilized. Furthermore, another COC microfluidic device was fabricated to store sperm and assess its quality parameters along time. The study herein presented demonstrates a good biocompatibility of the COC when working with gametes and it exhibits certain advantages such as the non-absorption of small molecules, gas impermeability and low fabrication costs –both at the prototyping and mass production scale, thus taking a step further towards fully automated microfluidic devices in ART.

Oocyte Maturation, Assisted Reproduction Techniques, Cyclic Olefin Co-polymer, Microfluidics, Hot Embossing

Introduction

Assisted reproductive technologies (ART) have enabled millions of people in the world to have children, who otherwise would not have been able to do so. The application of ART in animals, mainly by artificial insemination (AI), had a great impact in the improvement of the efficiency of animal production. Reproductive biotechnologies intend to be used routinely to shorten generational intervals and to propagate genetic material among breeding animal populations.¹ To achieve this goal, reproductive technologies have been developed over the years, for instance AI, embryo transfer, *in vitro* fertilization (IVF) and *in vitro* embryo production, and multiplication techniques (cloning) for the application of transgenesis.¹

Despite the remarkable progress made and the punctual relevance of some of the above-mentioned technologies, the efficiency of the processes is usually very low with the exception of AI in cattle. Furthermore, ART such as oocyte maturation or IVF require labor-intensive, time-consuming procedures (including frequent pipetting of oocytes to be washed, media changes, etc., which have not significantly evolved since their establishment) and some critical steps that only highly specialized personnel are able to perform.

Microfluidics has emerged as a new tool for ART that could potentially solve these problems by automating the handling and preparation procedures,² thus minimizing the errors associated to manual operation and reducing manipulation stress on the cells. Microfluidics can also provide environments that mimic *in vivo* conditions since fabrication technologies enable the design of structures resembling biological environments,³⁻⁶ including those related with ART.⁷ Furthermore, other inherent advantages of microfluidics, such as the low volumes required, the precise control of fluids or the miniaturization and integration of different elements in portable devices would also benefit ART.

The vast majority of microfluidic systems used in ART are made of polydimethylsiloxane (PDMS), a transparent and gas-permeable elastomer. This responds to its widespread use in the academia, which is due to several factors: cheap, rapid and easy prototyping, optical transparency, easy surface modification, elasticity, etc.⁸ The latter also provides the grounds for the integration of actuation systems, such as pumping or valving. ART applications of PDMS devices range from sperm separation,⁹ to oocyte fertilization¹⁰ or embryo culture,¹¹ among others. A comprehensive review of microfluidic systems applied in ART can be found in Swain *et al.*¹²

However, certain limitations of PDMS have hard-pressed the use of other materials in microfluidics, such as the thermoplastics.¹³ Among these, polystyrene (PS) and cyclic olefin co-polymers (COC) have emerged as alternatives for the production of microfluidic devices for biological applications, overcoming the limitations of PDMS. On the one hand, PS has been the choice material for disposable cell culture labware since the 1960s, and recently has been used as a substrate material to produce microfluidic devices,¹⁴ thus bringing together state of the art microfluidics technology and a well known material for biologists. However, the fabrication process is still challenging, mostly due to bonding issues.¹⁵

On the other hand, COC are a relatively new group of polymers with very promising properties for microfluidic applications,¹⁶ such as chemical resistance (higher than most thermoplastics), excellent optical transparency (even in the near UV region), low water absorption and biological compatibility.^{17,18} Furthermore, COC has obtained the *USP Class VI* qualification¹⁹ and is approved for use in medical devices. COC is a copolymer consisting of ethylene and norbornene, which offers several grade variations in terms of glass transition temperatures (T_g), ranging from 70 to 155 °C.²⁰ This is a big advantage in front of other thermoplastics, as it allows the bonding of different layers without channel deformation using grades with low T_g as sealants,²¹ and avoiding processes like solvent bonding, which are potentially harmful for biology applications. COC also enables surface modification,²² which can be useful to avoid protein adsorption, for instance in bioanalytical applications. Several fabrication techniques are available for the production of COC microfluidic devices, such as micromilling, hot embossing, injection molding, etc. The last two techniques enable the fabrication of the required microstructures to trap oocytes. However, the fabrication of the master is usually expensive and requires of relatively complex manufacturing processes such as photolithography.

Herein, we developed a new fabrication methodology combining CNC micromilling and hot embossing using LTCC masters, which enables fast prototyping as well as the fabrication of microfluidic features in the 50 to 100 μm range. Furthermore, we studied for the first time the suitability of a COC monolithic microfluidic device for an ART application. We studied bovine oocyte maturation and sperm characteristics during the culture in a COC microfluidic device. We investigated whether oocytes maintain the same rates of *in vitro* maturation and their ability to be fertilized. We also evaluated spermatozoa relevant parameters, such as viability, motility and membrane integrity, after culture in the microfluidic device. This is, to the best of our knowledge, the first COC monolithic microfluidic device dedicated to an ART application and from the obtained results we can

demonstrate the great potential of COC as a substrate material due to its biocompatibility and simple fabrication processes, both at the prototyping and mass production scales.

Materials and Methods

Reagents

All reagents were purchased from Sigma Chemical Co. (St. Louis, MO, USA) unless otherwise stated. Plastic dishes, four-well plates and tubes were obtained from Nunc (Roskilde, Denmark).

Fabrication of Microfluidic Devices

Two different microfluidic devices were fabricated on COC to separately study the maturation of oocytes and sperm storage. COC was obtained from TOPAS Advance Polymers GmbH (KY, USA). TOPAS 5013 sheets (T_g 134 °C) were used in this study for the machining of microchannels, while 25 μ m thick TOPAS 8007 foils (T_g 78 °C) were used as sealing substrate between layers using a temperature diffusion bonding technique, as described elsewhere.²³

Sperm storage microfluidic device

The fabrication procedure of this device is based on a procedure previously reported in our research group.²⁴ Briefly, the device consists of three layers of TOPAS 5013 1 mm thick. The top and bottom layers were laminated with a 25 μ m TOPAS 8007 (which acted later as glue to seal the device)²³ in a uniaxial hydraulic press (Talleres Francisco Camp, Granollers, Spain). The COC layers were machined using a micromilling Computer Numerically Controlled (CNC) machine Protomat S63 (LPKF Laser & Electronics, Garbsen, Germany). The fluidic channel was milled in the middle layer, by cutting the COC through. The top layer was drilled to create the inlets. Then, the three layers were aligned and laminated at 100 °C under a pressure of 6 bar. This approach prevents any surface roughness created by the milling machine when creating a bas-relief channel.

Oocyte-trapping microfluidic device

The oocyte-trapping microfluidic device was fabricated using a combination of hot embossing and micromilling. The microchannels that retain the oocytes were fabricated by means of a hot embossing technique in order

to obtain a “filter-like” structure with the appropriate dimensions to trap the oocytes –micromilling is not suitable for such dimensions– while the bigger features were machined using the CNC micromilling machine. Fig. 1 shows a schematic representation of the fabrication process.

Firstly, a master was built using Low Temperature Co-fired Ceramics (LTCC) 951PX, 254 μm thick, from Dupont (Germany). 8 LTCC layers were thermo-laminated together in a uniaxial hydraulic press. Then, the ceramic block was etched by means of a Protolaser 200, from LPKF (Garbsen, Germany) and sintered in a programmable box furnace from Carbolite (CBCWF11/23P16, Afora, Spain). The master was designed to have four negative images of microchannels, in order to create a filter-like structure in the microfluidic device.

Secondly, the LTCC master was used to fabricate the oocyte-trapping microfluidic device. A 500 μm thick layer of TOPAS 5013 was embossed with the master at 155 $^{\circ}\text{C}$ and 6 bar, thus obtaining four microchannels in the COC. Another 500 μm COC layer (previously laminated with a 25 μm thick TOPAS 8007 foil) was laminated with the replica, at 92 $^{\circ}\text{C}$ and 6 bar, to seal the microchannels and obtain the filter-like structure. The rest of the fluidic structures, namely the maturation chamber and the inlet/outlet channels, were machined cutting through the whole COC block using the micromilling machine.

The COC block with the microfluidic structures was thermally laminated between two more layers of COC (top and bottom layers), thus obtaining the sealed microfluidic device. Both top and bottom layers had been pre-laminated with a film of TOPAS 8007, which acted as gluing layer, as described elsewhere.²³ Inlet/outlet vias were drilled using the CNC micromilling machine.

Experimental design and setups

In order to evaluate the suitability and biocompatibility of COC as a substrate material for microfluidic devices used in ART, we designed two different microfluidic devices, one for sperm storage and another one for oocyte maturation. Three different sets of experiments were carried out.

Firstly, bovine oocytes were randomly distributed between the microfluidic device and a four-well culture dish, and matured for 24 h. Maturation rates were analyzed following nuclear and cytoplasmic maturation (chromosome and cortical granule distribution, respectively) by means of staining. Secondly, sperm viability, acrosome abnormalities and motility were assessed at 3, 6, 12 and 24 h in three different units, namely the sperm storage

microfluidic device, a four-well culture dish and a 1.5 mL Eppendorf tube. Finally, bovine oocytes were matured either in the microfluidic device or in a four-well culture dish, and subsequently fertilized *in vitro* in four-well dishes to evaluate penetration rates. All the experiments were conducted in triplicate.

In order to carry out these sets of experiments, two different setups were designed. On the one hand, the experiments involving the sperm storage microfluidic device were carried out by simply using a pipette to inject or retrieve the sperm samples into/from the device.

On the other hand, the experiments involving the oocyte-trapping microfluidic device were carried out in a setup schematically depicted in Fig. 2. Inlet 1 was connected to a syringe pump (540060, TSE Systems, Bad Homburg, Germany) in combination with a 2.5 mL gas-tight glass syringe from Hamilton (Bonaduz, Switzerland) by means of polytetrafluoroethylene (PTFE, i.d. 0.8 mm) tubing. This syringe (S1) contained the maturation medium to fill the microfluidic channels. Inlet 2 contained a short fragment of flexible Tygon tube, which was used as injection port for the polished glass capillary syringe (S2) containing the oocytes. Once the capillary was inserted in the injection port, the syringe was set on a pump in order to inject the oocytes into the microfluidic device. Port 3 was used as auxiliary waste outlet during the process of filling the device with media in order to remove any air bubbles, and then was capped with a stopper for the rest of the experiment. Port 4 was linked to a 3-way valve (161T031 NResearch, MA, USA) connecting the oocyte-trapping microfluidic device to either the waste (during oocytes loading) or a syringe (S4) with media (during oocyte collection after the experiment).

Bovine oocyte collection and in vitro maturation

Bovine ovaries were collected from recent culled dairy heifers at local slaughterhouses and immediately transported to the laboratory. They were then washed 3 times in warm saline solution (38 °C). Subsequently, follicles with a diameter of 2-6 mm were aspirated using an 18-gauge needle. Only unexpanded cumulus oocyte complexes surrounded by five or more cumulus cell layers and with homogeneous cytoplasm were matured *in vitro* and cultured at 38.5 °C in a humidified atmosphere of 5 % of CO₂ for 24h. The maturation medium contained TCM-199 medium supplemented with 10% (v/v) fetal calf serum, 10 ng/mL epidermal growth factor and 50 µg/mL gentamycin.²⁵

Assessment of sperm parameters

Commercial frozen bull semen of proven fertility was used. Semen straws were thawed in a water bath at 38.5 °C for 30 s and then spermatozoa were immediately centrifuged at room temperature in a top layer solution of a discontinuous gradient (BoviPure®, Nidacon International AB, Göthenborg, Sweden) for 10 min and $100 \times g$. The supernatant was removed, the pellet resuspended in 3 mL of BoviPure® wash solution and centrifuged again for 5 min at $100 \times g$. Sperm concentration of the pellet was determined using a haemocytometer chamber (Neubauer chamber) and adjusted to a final concentration of 1×10^6 spz/mL with fertilization medium (Tyrode's medium supplemented with 25 mM sodium bicarbonate, 22 mM sodium lactate, 1 mM sodium pyruvate, 6 mg/mL fatty acid-free bovine serum albumin (BSA) and 10 mg/mL heparin sodium salt [Calbiochem, Darmstadt, Germany]), and cultured at 38.5 °C in a humidified atmosphere of 5% of CO₂ for 24 h.

The sperm cells viability and acrosome abnormalities were assessed by the nigrosine-eosin stain method.²⁶ Ten microliters of sperm sample and 10 µL of the dye solution were mixed and smeared onto a glass slide and allowed air-drying. Then, the slide was covered with mounting medium and a cover glass. Slides were analyzed using an optical microscope (Motic BA210, Spain) at 1000x magnification under immersion oil. As many as 200 cells were counted on each slide and the percentage of sperm viability and spermatozoa with acrosome abnormalities were calculated.

The motility characteristics of the frozen-thawed spermatozoa were determined using a computer-assisted sperm analysis system (CASA system; Integrated Sperm Analysis System V1.2; Proiser SL, Valencia, Spain). The CASA system is based on the analysis of 25 consecutive digital images taken from a single field at 100x magnification in a dark background in a time lapse of 1s. A sample drop of 5 µL was placed on a prewarmed slide and viewed in a phase contrast microscope equipped with a warmer stage at 37 °C. At least five separate fields were taken of each sample and a minimum of 200 cells per sample were examined. The motility descriptors obtained after CASA were: progressive motility (percentage of spermatozoa that showed an average path velocity [VAP] above 50 µm/s and 70 % of straightness coefficient) and total motility (percentage of spermatozoa that showed a VAP above 10 µm/s).

Oocytes and sperm handling on-chip

The microfluidic devices were washed with 70 % ethanol and rinsed twice with Milli-Q water. After drying, they were exposed to UV light for 30 min for sterilization. Prior to introduction of either oocytes or sperm, the microfluidic devices were respectively filled in with maturation or fertilization medium equilibrated at 38.5 °C in a 5 % CO₂ incubator.

Oocytes were loaded into the microfluidic device through a flexible Tygon tube (Port 2, Fig 2), which acted as an injection port, where the tip of the polished glass capillary syringe S2 was inserted. Then, the syringe was coupled to a pump and a flow rate of 50 µL/min was applied until the oocytes reached the maturation chamber. To achieve that, Port 3 was capped and therefore the flow was directed from Port 2 to Port 4 through the filter-like microchannels, and then into the waste (see Fig. 2). The oocytes were thus retained in the filter-like structure since their size is bigger than the microchannel dimensions. In order to retrieve the oocytes after the maturation experiments, the flow direction was inverted: the syringe in Port 2 was unplugged –leaving only a small fragment of tube– and the valve in Port 4 was switched, connecting the device to the syringe S4. Then, a 50 µL/min flow rate was applied in the direction from Port 4 towards Port 2 (Fig. 2). Oocytes were thus collected in four-well plates.

Sperm samples were injected into the sperm storage microfluidic device directly with a pipette. Immediately after injection, both inlet and outlet were sealed using an adhesive film AB-1170 from Thermo Scientific (Schwerte, Germany), and the microfluidic device was incubated at 38.5 °C for the corresponding period of time. After the incubation, the film was removed and the sperm sample was collected with a pipette. The sperm samples were then analyzed to assess sperm quality parameters after exposure to the COC.

In vitro fertilization

After maturation, the cumulus oocyte complexes were washed twice in phosphate buffered saline solution (PBS) and then they were transferred to fertilization medium. Frozen-thawed bull spermatozoa were counted in a Neubauer chamber and diluted in an appropriate volume of fertilization medium to give a final concentration of 10⁶ spermatozoa/mL. All cumulus oocyte complexes were co-incubated with spermatozoa for 20 h at 38.5 °C in fertilization medium in a humidified 5 % CO₂ incubator.

Oocyte evaluation and classification

After 24 h of *in vitro* maturation, oocytes were totally denuded of cumulus cells by gentle pipetting in PBS. In order to evaluate nuclear stage and cortical granule distribution after *in vitro* maturation, oocyte samples were fixed in a solution of 4 % (w/v) of formaldehyde and PBS at 38.5 °C for 30 min and permeabilized in Triton X-100 2.5 % (v/v) in PBS for 15 min. Then, oocytes were immunostained for cortical granules detection with fluorescein isothiocyanate-labeled *Lens culinaris agglutinin* (FITC-LCA). Fixed and stained oocytes were mounted on poly-L-lysine treated coverslips fitted with a self-adhesive reinforcement ring in a 3 µl drop of Vectashield containing 125 ng/ml of 4',6-diamidino-2-phenylindole (DAPI) (Vectorlabs, Burlingame, CA) for chromosome detection and flattened with a coverslip. The preparation was sealed with nail varnish and stored at 4 °C protected from light. Chromosomes and cortical granules status of each oocyte were assessed under an epifluorescent microscope (Nikon Eclipse TE 2000S) and a laser-confocal microscope (Leica TCS SP2). Oocyte images were recorded in a computer.

Cultured oocytes were checked to have reached the metaphase II (MII) stage. Oocytes that reached the MII stage after maturation were classified into two categories: (1) Normal MII: Uniform alignment of the chromosomes on the spindle; (2) Anomalous MII: Nuclear content changed into chromatin-like structure forming condensed aggregates, forming aberrantly distributed chromosomes or absence of chromosomes.

Translocation of cortical granules to the oolema was used as an indicator of cytoplasmic maturation.²⁷ The criteria used to define the cortical granules distribution of oocytes was classified as two categories: (1) Normal cytoplasmic maturation: cortical granules were distributed adjacent to the plasma membrane and positioned such that they formed a continuous layer; (2) Anomalous cytoplasmic maturation: cortical granules appeared aggregated in clusters, or cortical granules were distributed in the cortical area (not limited to the vicinity of the plasma membrane), or absence of cortical granules.

Evaluation of sperm penetration

At 20 h post-insemination, the presumptive zygotes were pipetted to remove excess sperm and cumulus cells, washed three times in PBS, fixed in 4 % (v/v) paraformaldehyde in PBS at 38.5 °C for 30 min, stained with Vectashield containing DAPI and mounted on glass slides. The number of pronucleus was assessed under an epifluorescence microscope (Axioscop 40FL, Carl Zeiss, Germany). Once stained, slides were examined and

parameters including penetration, monospermic penetration, male pronucleus formation, and polyspermic penetration were recorded. Penetration was determined by the presence of one or more swollen sperm heads and/or male pronuclei. The presence of three or more pronuclei was designated as polyspermic.

Statistical analysis

All statistical analyses were performed using R program (version 2.15.0; R development Core Team, 2009). Data of *on-chip* oocyte maturation were analysed using contingency tables and Pearson's Chi-squared statistical test. The analysis of differences among the different tested devices for sperm viability and motility parameters was carried out using the Kruskal-Wallis test. All data are expressed as mean \pm SD. In all cases, differences between groups with $P < 0.05$ were considered significant.

Results and discussion

Microfluidic design and fabrication

Two different microfluidic devices were designed in order to study the oocytes and the sperm samples independently. The microfluidic device for sperm consisted of a simple channel to store the sperm for different periods of time and then compare the quality of the samples with the control experiments. Four independent microfluidic units were fabricated on the same substrate to study the sperm samples at 3, 6, 12 and 24 hours, respectively. The dimensions of the channel were chosen to fit the required volume for the motility and viability tests, plus excess in case it might be needed (total volume *ca.* 90 μ L). Fig. 3 shows the microfluidic device used in the study of the sperm samples.

The oocyte-trapping microfluidic device consisted of a maturation chamber with a filter-like structure to trap the oocytes and four inlet-outlet ports (see Fig. 4). The auxiliary ones (ports *Aux. In* and *Aux. Out*) were used to fill the entire device with the maturation medium and remove any air bubble prior to oocyte introduction. The features of the oocyte microfluidic device were more challenging than those of the sperm microfluidic device, from the fabrication perspective. Microfluidic channels with a smaller size than the oocyte diameter were required to trap them, and common micromilling equipment, usually employed for thermoplastics, is not able to achieve such dimensions.²⁸ Therefore, filter-like channels were hot embossed on the COC plates.

Several materials can be found in the literature for the fabrication of masters, e.g. micromilled brass,²⁹ photolithographically patterned silicon³⁰ or epoxy.¹⁸ However, the fabrication of these type of masters require time-consuming and expensive processes. Therefore, the master used in this work was fabricated using LTCC technology, due to its simple and fast iteration from design to prototype (around 6 hours) in an inexpensive way.³¹ Furthermore, no clean room facilities were required for its fabrication. Several COC replicas were fabricated without noticeable degradation of the master. The simple prototyping enabled by the LTCC technology enhances the optimization process of the master features required by the desired application.

The different layers of COC were laminated together using the thermal diffusion bonding technique. TOPAS 8007 foils, 25 μm thick, were used as “gluing” layer. The lower T_g of this substrate enables the lamination of the layers with minimal deformation. In this case, this is particularly important in order to avoid occlusion due to the reduced dimensions of the filter-like microchannels. The availability of a number of COC grades with different thermal properties is one of its assets in front of other thermoplastics like polystyrene for several reasons: the fabrication process becomes simpler, smaller features can be implemented in monolithic devices and surface modification/activation or solvents are not required for bonding. The latter fact is very important in biological applications, since solvents and other reagents used for surface modification could potentially harm cells.

The filter-like microchannels obtained after sealing the microfluidic device had a trapezoidal shape, with dimensions of approximately 100 and 50 μm respectively for the bases, and 55 μm high (see Fig. 4 C). The oocyte-trapping microfluidic device enabled the injection, maturation and removal of the oocytes (see Fig. 5).

On-chip oocyte maturation

The oocytes were injected into the microfluidic device at an optimal flow rate of 50 $\mu\text{L}/\text{min}$ (experimentally determined). Using smaller flow rates would involve longer times for oocyte loading/retrieval. No oocyte deformation was observed using this flow rate. Higher flow rates would cause deformation and/or denudation of the oocytes in the filter-like channels (channel constriction). Other studies in the literature take advantage of this phenomenon for cumulus removal.³² However, we were not interested in it due to the important role of cumulus cells in oocyte maturation.³³ The oocytes were retained in the vicinity of the filter-like microchannels of the maturation chamber, as seen in Fig. 5.

Fig. 6 A shows the results obtained from the oocytes *in vitro* matured into the microfluidic device compared to the four-well culture dish. Fig. 6 B and C show examples of oocytes correctly matured. Although oocytes matured in the microfluidic device showed a low-grade cumulus cell expansion, no significant differences ($P>0.05$) were found in the percentage of oocytes progressing to normal MII and cytoplasmic maturation between both devices. These results are in agreement with others found in the literature³⁴ in which pig oocytes matured in PDMS microchannels did not show significant differences ($P>0.05$) in the percentage of maturation rates as compared with oocytes matured in conventional 500 μL drops or in 8 μL drops (volume control). In addition, Walters *et al.*³⁴ also observed a low grade of cumulus cell expansion of the cumulus-oocyte complexes matured in the PDMS device. The molecular processes involved in cumulus cell expansion need to be evaluated to check presumptive implications on processes related to fertilization and embryo development.

The small volumes used in microfluidics may lead to a rapid depletion of factors and/or a pH shift in the surroundings of the oocytes. The pH in the microfluidic device is not buffered with the CO_2 atmosphere of the incubator because it is airtight –unlike the four-well dish– and this could cause the lower cumulus cell expansion, since oocytes appear to lack porters to regulate their intracellular pH,^{35,36} which is greatly affected by CO_2 and O_2 concentrations.³⁷ Although this could be overcome by employing dynamic culture, *i.e.* imparting flow and thus renewing the media, in this study we evaluated the static culture as it can be more easily compared to the traditional four-well dish method.

Time dependent on-chip sperm evaluation

Results obtained from the analysis of the sperm storage into the microfluidic device, a four-well culture dish and a 1.5 mL Eppendorf tube are shown in Table 1. Data show the expected decrease of the percentage of viability and motility, and an increase of the percentage of acrosome abnormalities along time with no significant differences among the three devices ($P>0.05$). This suggests that COC is an innocuous and biocompatible material regarding sperm quality parameters, and it could be used for the development of microfluidic systems. Previous studies have tested biocompatibility of materials such as polystyrene (standard Petri dish material), polyimides, silicons and PDMS assessing mice embryo development and pig sperm motility parameters.^{38–40} However, to the authors' best knowledge, this is the first study that has tested the biocompatibility and absence of toxicity of COC on bovine gametes.

Table 2 shows the significant higher percentages of sperm penetration observed in the four-well culture dish when compared to the microfluidic device at 18 h after IVF (61.44 % vs. 35.63 %, respectively; $P < 0.05$). However, in terms of normal fertilization with male pronuclear formation, no significant differences were observed between both devices ($P > 0.05$). These data suggest that when an oocyte is penetrated by a sperm cell, fertilization is comparable and efficient in both maturation systems. Thus, the detected reduction in the fertilization rate after *on-chip* oocyte maturation seems to be a consequence of the quality of the matured oocyte more than due to deficiencies in the process of fertilization. The oocyte maturation system adequately supported nuclear maturation but probably failed to produce oocytes with a complete cytoplasmic competency, additionally to correct cortical granules migration and maturation. Cytoplasmic maturation encompasses a wide array of metabolic and structural modifications, including events that ensure the occurrence of normal fertilization, meiotic to mitotic cell cycle progression, and activation of pathways required for genetic and epigenetic programs of preimplantation embryonic development.⁴¹ Additionally, it is known that cumulus cell expansion is an important marker for oocyte maturation.⁴² Indeed, in cattle, inhibition of cumulus cell expansion was shown to be independent from nuclear maturation, but essential for fertilization and subsequent cleavage and blastocyst development.⁴³ Thus, it might be thought that the low-grade of cumulus cell expansion observed after *on-chip* maturation could also be related to a poorer maturation of the zona pellucida, necessary for a proper fertilization of the oocyte. However, and as stated before, employing a dynamic culture with the *on-chip* oocyte maturation system could help to improve the overall oocyte maturation.

The differences between the microfluidic device and the four-well culture dish can also be explained by the fact that the COC microfluidic device is airtight and does not allow the gas exchange, thus impeding the buffering of the media by the CO_2 contained inside the incubator. Similar maturation studies in PDMS microfluidic devices (gas permeable) show a significantly higher percentage of porcine embryo cleavage rates (67 % vs. 49 %; $p < 0.05$).⁴⁴ However, the gas permeability of PDMS implies that the microfluidic device needs to be in an incubator with controlled atmosphere. In contrast, COC microfluidic devices in combination with a suitable heater^{45,46} would not require a control of the atmosphere, and therefore minimize the required equipment. Moreover, the problem of the depletion of factors around the oocytes and the media buffering could be overcome by using a dynamic culture, *i.e.* renewing the media by pumping fresh one into the maturation chamber.

Conclusions

This work describes a novel rapid prototyping process for COC microfluidic devices, combining a hot embossing step –using an LTCC master– for the smaller features required and a micromilling step for the rest of the fluidic structures. We have demonstrated that the COC microfluidic device enables the functional and automated maturation of oocytes and that it is non-toxic for gametes. The microfluidic device allows trapping the oocytes by means of a filter-like structure and their maturation. No significant differences were observed in oocytes reaching normal MII and cytoplasmic maturation in terms of cortical granules migration, compared to the control experiments. Lower penetration rates were observed for oocytes matured in the microfluidic device, which could be related to the lower grade of cumulus cell expansion of the cumulus-oocyte complexes or an incomplete cytoplasmic maturation of the oocytes. However, this issue could be addressed by improving the factor availability and pH buffering capacity in the surroundings of the oocytes, for instance, by dynamic culture.

The properties of COC open new possible applications for microfluidic systems in ART due to the simple fabrication processes both at the prototyping and mass-production scales, taking advantage of the different material grades commercially available. COC is not hindered by mass production limitations, absorption of molecules or gas permeability, thus avoiding a strict control of the exterior atmosphere conditions, and provides simpler fabrication methods than other thermoplastics, especially regarding bonding.

Current efforts focus, on the one hand, on the development of a temperature control system to avoid the use of big, heavy and expensive equipment such as incubators, and on the other hand, on the control of the factors and the buffering of the media in the surroundings of the oocytes. These two features would enable the construction of an independent automated microfluidic platform using COC for different ART applications.

Acknowledgements

The authors gratefully acknowledge the financial support of the Ministerio de Economía y Competitividad and FEDER (projects CTQ2012-36165 and AGL2013-46769-P) and by the Government of Catalonia (SGR 2014-837). M. Berenguel-Alonso was supported by the Government of Catalonia with a scholarship FI-DGR 2012, co-funded by the ESF). M. Sabés-Alsina was supported by a Predoctoral Research Fellowship (PIF) from the Universitat Autònoma de Barcelona, Bellaterra, Spain. R. Morató was supported by a Postdoctoral Research Fellowship ('Juan de la Cierva' Scheme; Ministry of Economy and Competitiveness, Spain).

References

1. Rodriguez-Martinez, H. Assisted Reproductive Techniques for Cattle Breeding in Developing Countries: A Critical Appraisal of Their Value and Limitations. *Reprod. Domest. Anim.* **2012**, *47*, 21–26.
2. Luo, Z.; Güven, S.; Gozen, I.; et al. Deformation of a Single Mouse Oocyte in a Constricted Microfluidic Channel. *Microfluid. Nanofluidics* **2015**, *19*, 883–890.
3. Ziółkowska, K.; Kwapiszewski, R.; Brzózka, Z. Microfluidic Devices as Tools for Mimicking the in Vivo Environment. *New J. Chem.* **2011**, *35*, 979.
4. Beebe, D. J.; Ingber, D. E.; den Toonder, J. Organs on Chips 2013. *Lab Chip* **2013**, *13*, 3447.
5. Rigat-Brugarolas, L. G.; Elizalde-Torrent, A.; Bernabeu, M.; et al. A Functional Microengineered Model of the Human Splenon-on-a-Chip. *Lab Chip* **2014**, *14*, 1715.
6. Auroux, P.-A.; Iossifidis, D.; Reyes, D. R.; et al. Micro Total Analysis Systems. 2. Analytical Standard Operations and Applications. *Anal. Chem.* **2002**, *74*, 2637–2652.
7. Kim, M. S.; Bae, C. Y.; Wee, G.; et al. A Microfluidic in Vitro Cultivation System for Mechanical Stimulation of Bovine Embryos. *Electrophoresis* **2009**, *30*, 3276–82.
8. Mukhopadhyay, R. When PDMS Isn't the Best. *Anal. Chem.* **2007**, *79*, 3248–3253.
9. Cho, B. S.; Schuster, T. G.; Zhu, X.; et al. Passively Driven Integrated Microfluidic System for Separation of Motile Sperm. *Anal. Chem.* **2003**, *75*, 1671–1675.
10. Ma, R.; Xie, L.; Han, C.; et al. In Vitro Fertilization on a Single-Oocyte Positioning System Integrated with Motile Sperm Selection and Early Embryo Development. *Anal. Chem.* **2011**, *83*, 2964–70.
11. Esteves, T. C.; van Rossem, F.; Nordhoff, V.; et al. A Microfluidic System Supports Single Mouse Embryo Culture Leading to Full-Term Development. *RSC Adv.* **2013**, *3*, 26451.
12. Swain, J. E.; Lai, D.; Takayama, S.; et al. Thinking Big by Thinking Small: Application of Microfluidic Technology to Improve ART. *Lab Chip* **2013**, *13*, 1213–24.
13. Sackmann, E. K.; Fulton, A. L.; Beebe, D. J. The Present and Future Role of Microfluidics in Biomedical Research. *Nature* **2014**, *507*, 181–9.
14. Young, E. W. K.; Berthier, E.; Guckenberger, D. J.; et al. Rapid Prototyping of Arrayed Microfluidic Systems in Polystyrene for Cell-Based Assays. *Anal. Chem.* **2011**, *83*, 1408–17.
15. Berthier, E.; Young, E. W. K.; Beebe, D. Engineers Are from PDMS-Land, Biologists Are from Polystyrenia. *Lab Chip* **2012**, *12*, 1224–37.
16. Nunes, P. S.; Ohlsson, P. D.; Ordeig, O.; et al. Cyclic Olefin Polymers: Emerging Materials for Lab-on-a-Chip Applications. *Microfluidics and Nanofluidics*, 2010, *9*, 145–161.
17. van Midwoud, P. M.; Janse, A.; Merema, M. T.; et al. Comparison of Biocompatibility and Adsorption Properties of Different Plastics for Advanced Microfluidic Cell and Tissue Culture Models. *Anal. Chem.* **2012**, *84*, 3938–44.
18. Jeon, J. S.; Chung, S.; Kamm, R. D.; et al. Hot Embossing for Fabrication of a Microfluidic 3D Cell Culture Platform. *Biomed. Microdevices* **2011**, *13*, 325–33.
19. Kuo, J. S.; Chiu, D. T. Disposable Microfluidic Substrates: Transitioning from the Research Laboratory into the Clinic. *Lab Chip* **2011**, *11*, 2656–65.
20. Tsao, C.-W.; DeVoe, D. L. Bonding of Thermoplastic Polymer Microfluidics. *Microfluid. Nanofluidics* **2008**, *6*, 1–16.
21. Jena, R. K.; Yue, C. Y.; Lam, Y. C. Micro Fabrication of Cyclic Olefin Copolymer (COC) Based Microfluidic Devices. *Microsyst. Technol.* **2011**, *18*, 159–166.
22. Jena, R. K.; Yue, C. Y. Cyclic Olefin Copolymer Based Microfluidic Devices for Biochip Applications: Ultraviolet Surface Grafting Using 2-Methacryloyloxyethyl Phosphorylcholine. *Biomicrofluidics* **2012**, *6*, 12822.
23. Steigert, J.; Haerberle, S.; Brenner, T.; et al. Rapid Prototyping of Microfluidic Chips in COC. *J. Micromechanics Microengineering* **2007**, *17*, 333–341.
24. Berenguel-Alonso, M.; Granados, X.; Faraudo, J.; et al. Magnetic Actuator for the Control and Mixing of Magnetic Bead-Based Reactions on-Chip. *Anal. Bioanal. Chem.* **2014**, *406*, 6607–16.
25. Rizos, D.; Ward, F.; Boland, M. P.; et al. Effect of Culture System on the Yield and Quality of Bovine Blastocysts as Assessed by Survival after Vitrification. *Theriogenology* **2001**, *56*, 1–16.
26. Bamba, K. Evaluation of Acrosomal Integrity of Boar Spermatozoa by Bright Field Microscopy Using an Eosin-Nigrosin Stain. *Theriogenology* **1988**, *29*, 1245–1251.

27. Damiani, P.; Fissore, R. A.; Cibelli, J. B.; et al. Evaluation of Developmental Competence, Nuclear and Ooplasmic Maturation of Calf Oocytes. *Mol. Reprod. Dev.* **1996**, *45*, 521–534.
28. Guckenberger, D. J.; de Groot, T.; Wan, A. M.-D.; et al. Micromilling: A Method for Ultra-Rapid Prototyping of Plastic Microfluidic Devices. *Lab Chip* **2015**.
29. Hupert, M. L.; Guy, W. J.; Llopis, S. D.; et al. Evaluation of Micromilled Metal Mold Masters for the Replication of Microchip Electrophoresis Devices. *Microfluid. Nanofluidics* **2006**, *3*, 1–11.
30. Charest, J. L.; Eliason, M. T.; García, A. J.; et al. Combined Microscale Mechanical Topography and Chemical Patterns on Polymer Cell Culture Substrates. *Biomaterials* **2006**, *27*, 2487–2494.
31. Ibáñez-García, N.; Alonso, J.; Martínez-Cisneros, C. S.; et al. Green-Tape Ceramics. New Technological Approach for Integrating Electronics and Fluidics in Microsystems. *TrAC Trends Anal. Chem.* **2008**, *27*, 24–33.
32. Zeringue, H. C.; Beebe, D. J.; Wheeler, M. B. Removal of Cumulus from Mammalian Zygotes Using Microfluidic Techniques. *Biomed. Microdevices* **2001**, *3*, 219–224.
33. Zhang, L.; Jiang, S.; Wozniak, P. J.; et al. Cumulus Cell Function during Bovine Oocyte Maturation, Fertilization, and Embryo Development in Vitro. *Mol. Reprod. Dev.* **1995**, *40*, 338–344.
34. Walters, E. M.; Beebe, D. J.; Wheeler, M. B. In Vitro Maturation of Pig Oocytes in Polydimethylsiloxane (PDMS) and Silicon Microfluidic Devices. *Theriogenology* **2001**, *55*, 497.
35. FitzHarris, G.; Baltz, J. M. Granulosa Cells Regulate Intracellular pH of the Murine Growing Oocyte via Gap Junctions: Development of Independent Homeostasis during Oocyte Growth. *Development* **2006**, *133*, 591–599.
36. Phillips, K. P.; Petrunewich, M. A. F.; Collins, J. L.; et al. The Intracellular pH-Regulatory HCO₃⁻/Cl⁻ Exchanger in the Mouse Oocyte Is Inactivated during First Meiotic Metaphase and Reactivated after Egg Activation via the MAP Kinase Pathway. *Mol. Biol. Cell* **2002**, *13*, 3800–3810.
37. Pinyopummintr, T.; Bavister, B. D. Optimum Gas Atmosphere for in Vitro Maturation and in Vitro Fertilization of Bovine Oocytes. *Theriogenology* **1995**, *44*, 471–477.
38. Chan, N. G.; Raty, S.; Zeringue, H. C.; et al. Development of Microfabricated Devices for Embryo Production: Embryo Biocompatibility. *Theriogenology* **2001**, *55*, 332.
39. Clark, S. G.; Davis, J.; Beebe, D. J.; et al. Biocompatibility of Porcine Sperm Cells in Polydimethylsiloxane (PDMS). *Theriogenology* **2001**, *55*, 421.
40. Chan, N. G.; Lyman, J. T.; Choi, S. J.; et al. Development of an Embryo Transport and Analysis System: Material Biocompatibility. *Theriogenology* **1999**, *51*, 234.
41. Combelles, C. M. H. Assessment of Nuclear and Cytoplasmic Maturation in in-Vitro Matured Human Oocytes. *Hum. Reprod.* **2002**, *17*, 1006–1016.
42. Chen, L.; Wert, S. E.; Hendrix, E. M.; et al. Hyaluronic Acid Synthesis and Gap Junction Endocytosis Are Necessary for Normal Expansion of the Cumulus Mass. *Mol. Reprod. Dev.* **1990**, *26*, 236–247.
43. Gutnisky, C.; Dalvit, G. C.; Pintos, L. N.; et al. Influence of Hyaluronic Acid Synthesis and Cumulus Mucification on Bovine Oocyte in Vitro Maturation, Fertilisation and Embryo Development. *Reprod. Fertil. Dev.* **2007**, *19*, 488.
44. Hester, P. N.; Roseman, H. M.; Clark, S. G.; et al. Enhanced Cleavage Rates Following in Vitro Maturation of Pig Oocytes within Polydimethylsiloxane-Borosilicate Microchannels. *Theriogenology* **2002**, *57*, 723.
45. Miralles, V.; Huerre, A.; Malloggi, F.; et al. *A Review of Heating and Temperature Control in Microfluidic Systems: Techniques and Applications*; 2013; Vol. 3.
46. Heo, Y. S.; Cabrera, L. M.; Bormann, C. L.; et al. Real Time Culture and Analysis of Embryo Metabolism Using a Microfluidic Device with Deformation Based Actuation. *Lab Chip* **2012**, *12*, 2240–6.

Tables and table legends

Table 1. Sperm quality parameters (viability, acrosome abnormalities and motility characteristics) after the storage in three different devices (microfluidic device, a four-well culture dish and a 1.5 mL Eppendorf tube) for 3, 6, 12 and 24 h.

Parameter	Time (h)	Microfluidic device	Four-well culture dish	Eppendorf tube
Viable sperm cells (%)	3	48.3 ± 3.0	52.8 ± 3.6	50.2 ± 4.5
	6	34.7 ± 5.5	37.7 ± 10.9	39.6 ± 8.5
	12	20.5 ± 0.5	29.1 ± 5.3	27.8 ± 6.1
	24	20.0 ± 8.2	27.0 ± 4.8	22.5 ± 3.1
Acrosome abnormalities (%)	3	44.8 ± 11.6	43.5 ± 19.8	37.2 ± 2.5
	6	46.3 ± 9.8	38.2 ± 7.7	48.0 ± 6.1
	12	70.5 ± 12.2	46.2 ± 17.4	52.5 ± 4.6
	24	70.5 ± 17.8	67.5 ± 9.9	66.7 ± 2.8
Progressive motility (%)	3	18.1 ± 0.5	15.9 ± 4.9	18.2 ± 0.6
	6	17.9 ± 5.0	19.4 ± 3.2	22.4 ± 7.6
	12	6.1 ± 4.8	12.5 ± 3.1	12.8 ± 7.2
	24	1.7 ± 0.5	5.7 ± 5.8	3.0 ± 1.3
Total motility (%)	3	28.9 ± 3.4	22.3 ± 3.9	24.0 ± 2.4
	6	27.2 ± 5.0	24.1 ± 3.9	27.2 ± 6.4
	12	11.1 ± 2.8	16.0 ± 3.2	16.7 ± 8.9
	24	4.1 ± 3.1	7.2 ± 6.4	4.2 ± 1.1

Table 2. Effects of devices on the *in vitro* fertilization rates of *in vitro* matured bovine oocytes.

Device	Oocytes (n)	Total fertilization	Normal fertilization	Abnormal fertilization
		Penetration (%)	Male pronucleus formation (%)	Polyspermic penetration (%)
Four-well culture dish	153	61.4*	82.9	17.0
Microfluidic device	87	36.8*	78.8	21.9

*Values within a column differ significantly, P<0.05.

Figures

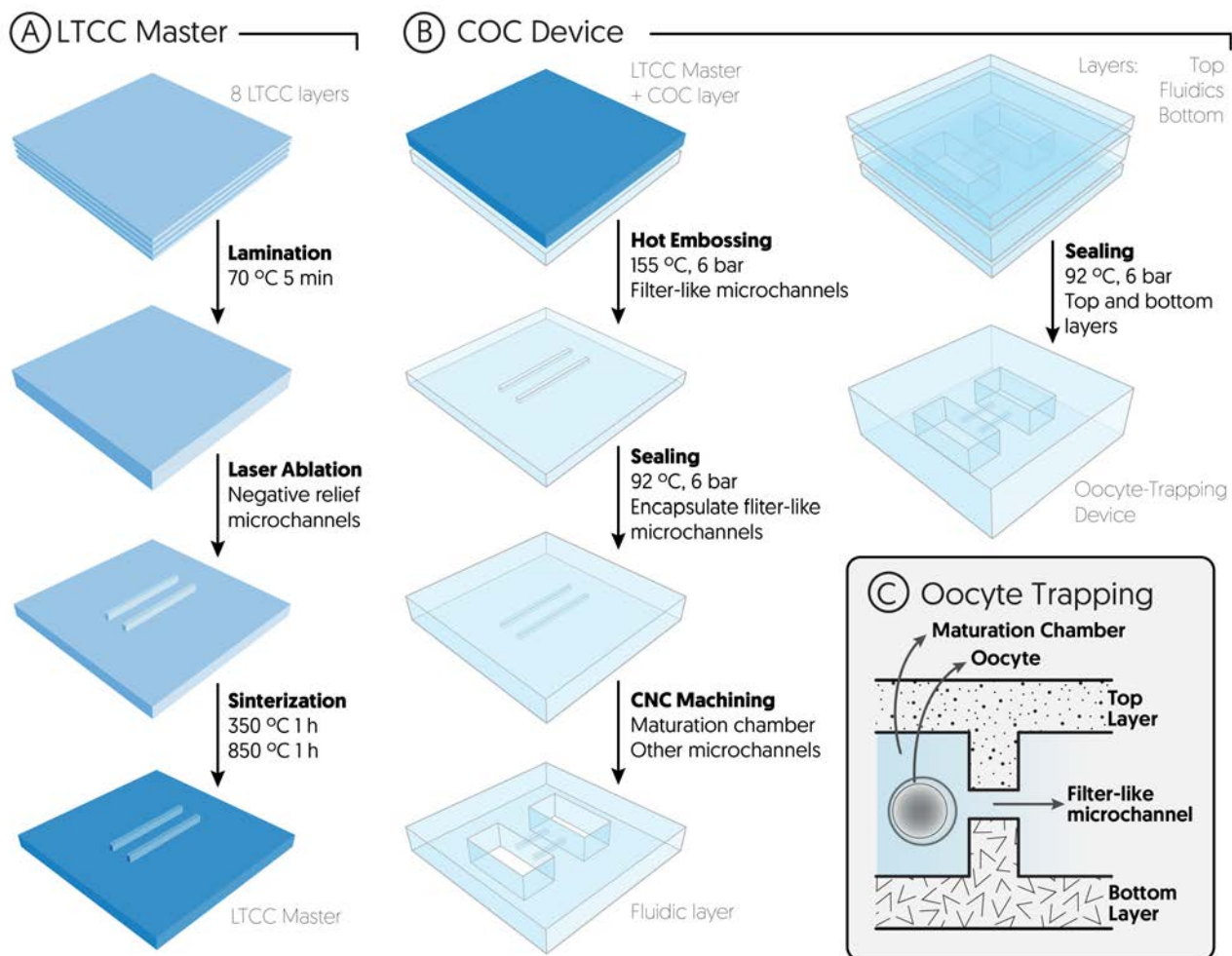


Fig. 1 Schematic representation (not to scale) of the oocyte-trapping microfluidic device fabrication and working principle of the entrapment. A) Fabrication of the LTCC master. B) Fabrication of the COC oocyte-trapping microfluidic device, by means of hot embossing the smallest features (*i.e.* the filter-like microchannels) and micromilling the maturation chamber and the rest of the channels. The device is then sealed by means of a thermo-compression process. C) Cross-section view of the device showcasing the oocyte trapping principle, which is based on a channel constriction where the oocytes do not fit –the oocytes are trapped in a filter-like structure.

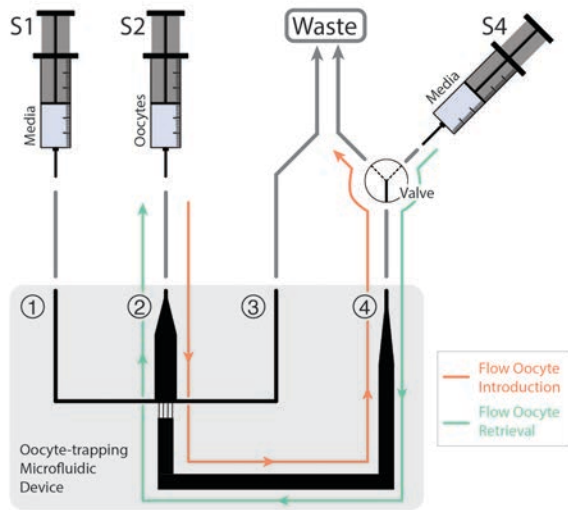


Fig. 2 Schematic representation of the experimental setup for the oocyte maturation experiments *on-chip*. The oocyte-trapping microfluidic device consisted of 4 inlet/outlet ports. Ports 1 and 3 were simply used to fill the device with media and remove any air bubbles trapped next to the filter-like channels. Ports 2 and 4 were used for the oocyte injection/retrieval.

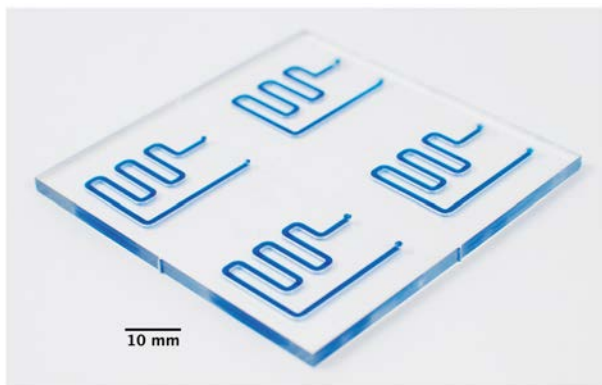


Fig. 3 Microfluidic device for sperm storage. The device features four independent fluidic units to analyze a sample at different times. For clarity purposes, the channels were filled with blue dye.

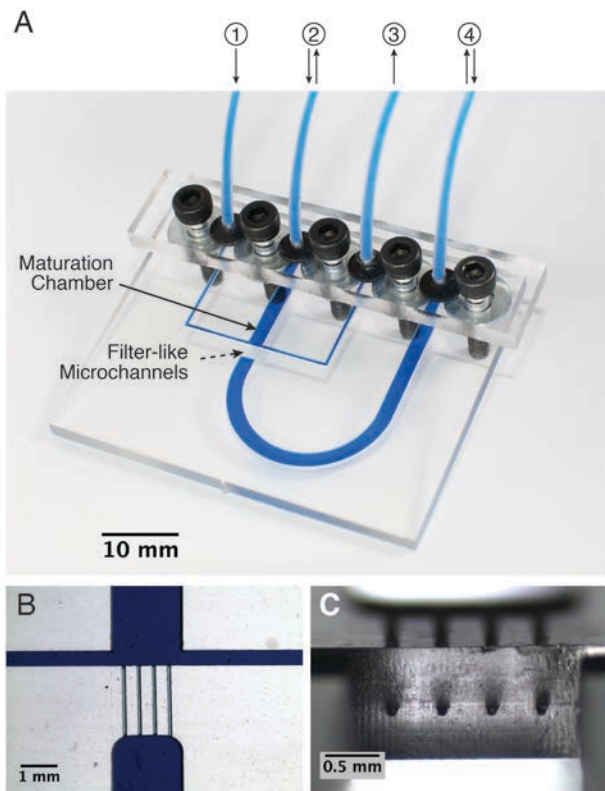


Fig. 4 A) Oocyte-trapping microfluidic device. The dashed arrow indicates the position of the capillary channels that act as a filter for oocytes. For clarity purposes, the channels were filled with blue dye. B) Microscope close-up of the oocyte-trapping region. C) Cross-section view of the oocyte-trapping microchannels embossed using the LTCC master.

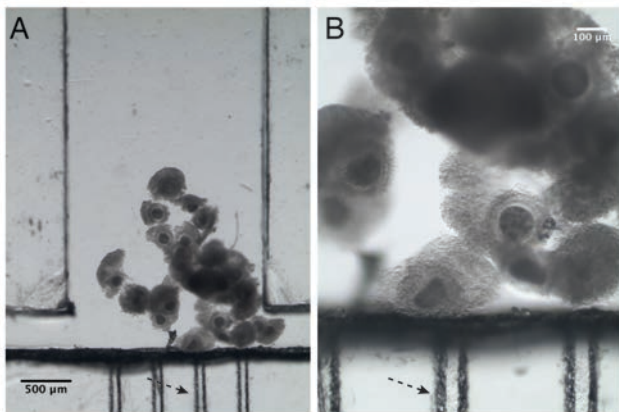


Fig. 5 Microscope pictures of the oocytes trapped in the microfluidic device. The dashed arrow indicates the position of the capillary channels that act as a filter for oocytes. A) General view of the maturation chamber and B) close-up of the oocytes near the capillary channels. The shadowed areas of the capillary channel correspond to its walls, as it has a trapezoidal shape.

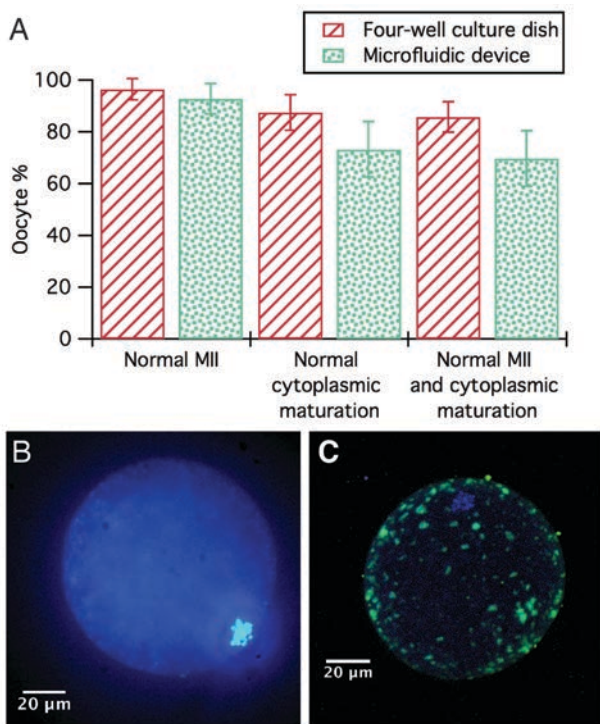


Fig. 6 A) Effect of different culture devices on nuclear and cytoplasmic maturation of bovine oocytes. No significant differences were detected ($P > 0.05$). B) Oocyte correctly matured in vitro to the Metaphase II nuclear stage. Image obtained under an epifluorescence microscope after DAPI staining. Oocyte diameter is close to 100 μm . C) Oocyte correctly matured in terms of nuclear maturation (MII stage) and cortical granules (CG) migration. Image merged from nuclear (blue fluorescence) and CG (green fluorescence) staining under confocal laser microscopy.